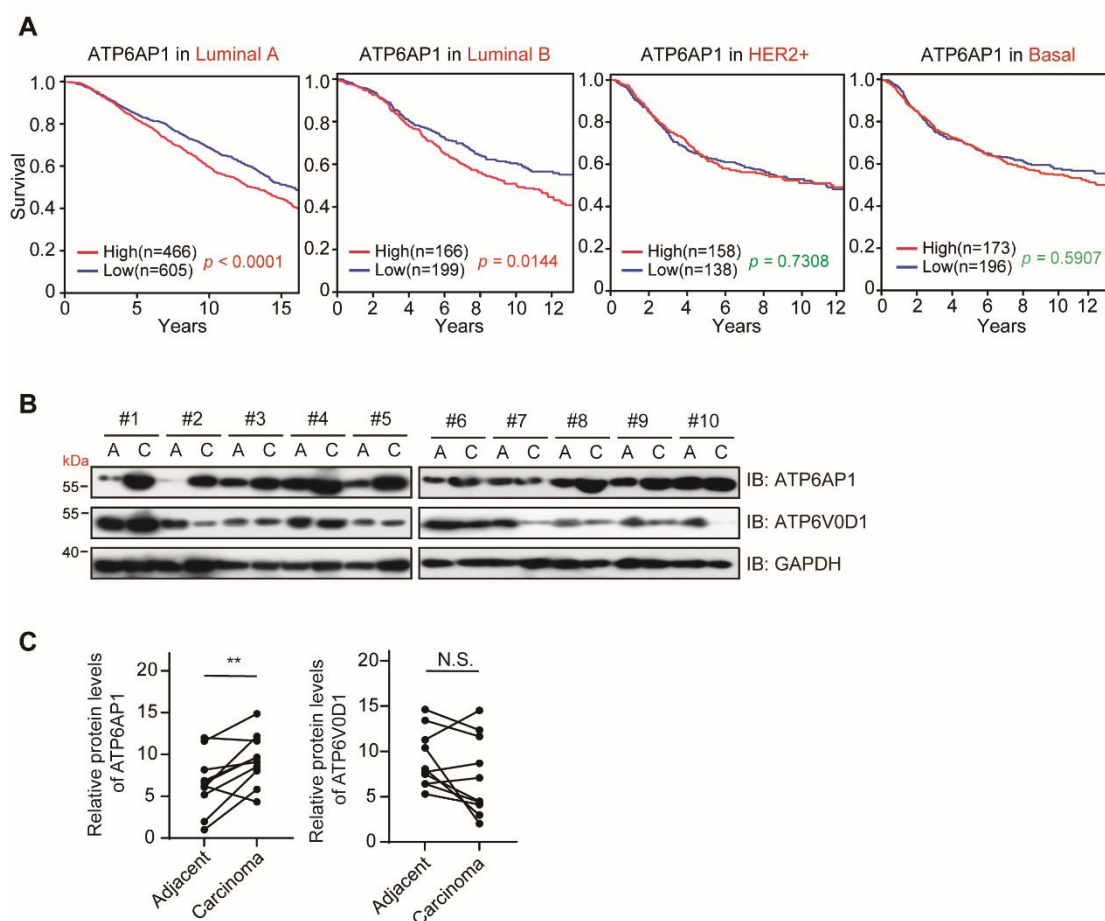


**Figure S1**



**Figure S1. Supplementary figure to Figure 1**

(A) Kaplan–Meier survival curve analysis of the prognostic significance of high and low expression of ATP6AP1 in different subclasses of breast cancer using the bc-GenExMiner tool.

(B and C) Western blotting analysis of ATP6AP1 and ATP6V0D1 expression in luminal breast cancer samples and matched adjacent breast tissue samples. A, adjacent tissue; C, carcinoma tissue.  $n = 10$ , \*\* $p < 0.01$ , N.S., no significance.

**Figure S2**

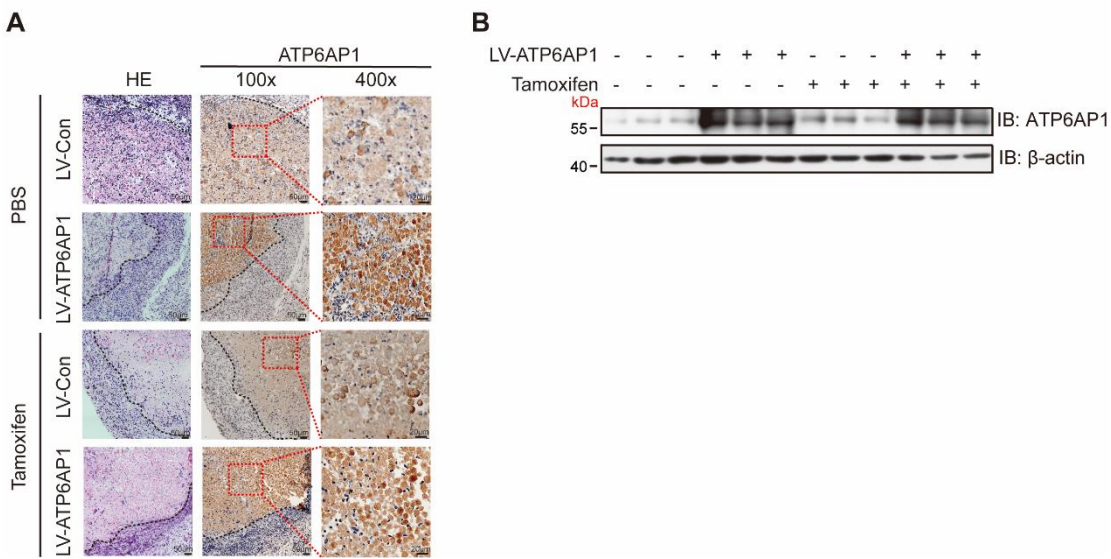


**Figure S2. Supplementary figure to Figure 2**

(**A and B**) Xenograft mouse models were developed using ZR-75-1 cells that stably overexpressed ATP6AP1 or contain an empty vector. The overexpression of ATP6AP1 was verified by IHC (**A**) and western blotting (**B**). Scale bars, 50  $\mu$ m (left), 20  $\mu$ m (right).

## Figure S3

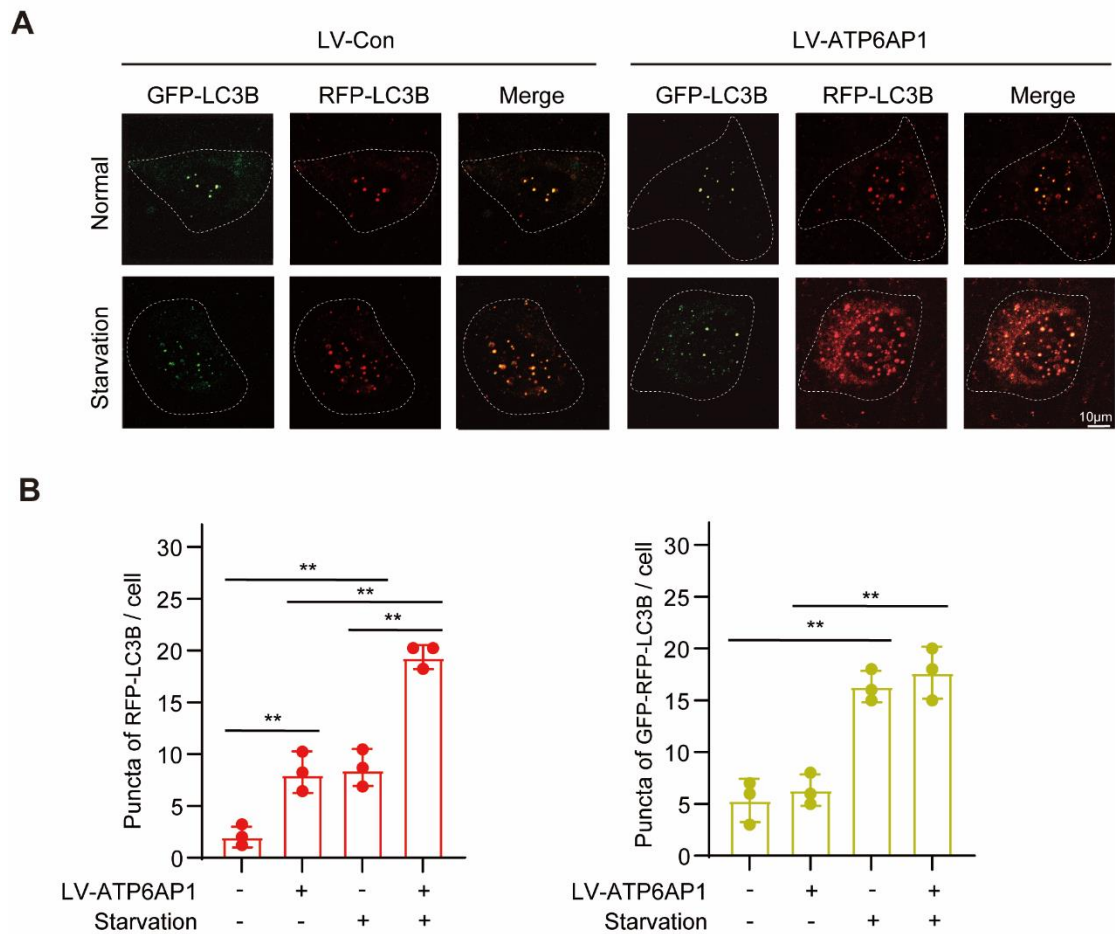


**Figure S3. Supplementary figure to Figure 4**

(A) T47D cells were transfected with LV-Con or LV-ATP6AP1 for 48 h and then treated with HBSS for 6 h. Green and red fluorescence was detected by confocal microscopy. Scale bars, 10  $\mu$ m.

(B) Quantification of autophagic flux as analyzed in (A). The average percentage of yellow puncta and red puncta per cell was calculated. The bar graph displays the mean $\pm$ SD, n=3, \*\* $p$ <0.01.

**Figure S4**

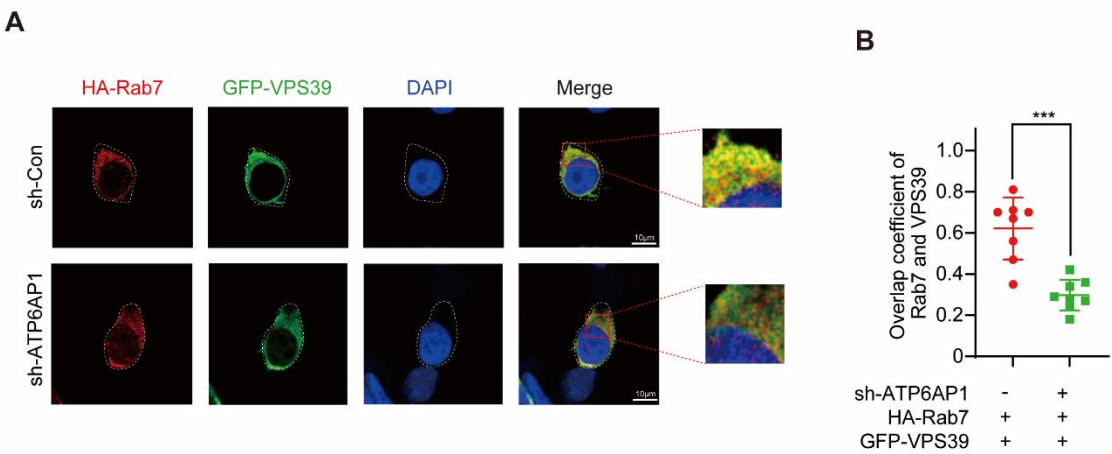


**Figure S4. Supplementary figure to Figure 5**

**(A)** The knockdown of ATP6AP1 reduces the co-localization of Rab7 with VPS39. Representative immunofluorescence images showing the co-localization of Rab7 and VPS39 in MCF-7 cells that were infected with Lv-sh-ATP6AP1 and transfected with HA-Rab7 and GFP-VPS39. Scale bars, 10  $\mu$ m.

**(B)** Quantification of Rab7-VPS39 colocalized voxels (volumetric pixels). Mean $\pm$ SD, \*\*\* $p$ < 0.001 by two-way ANOVA (n =8).

**Figure S5**

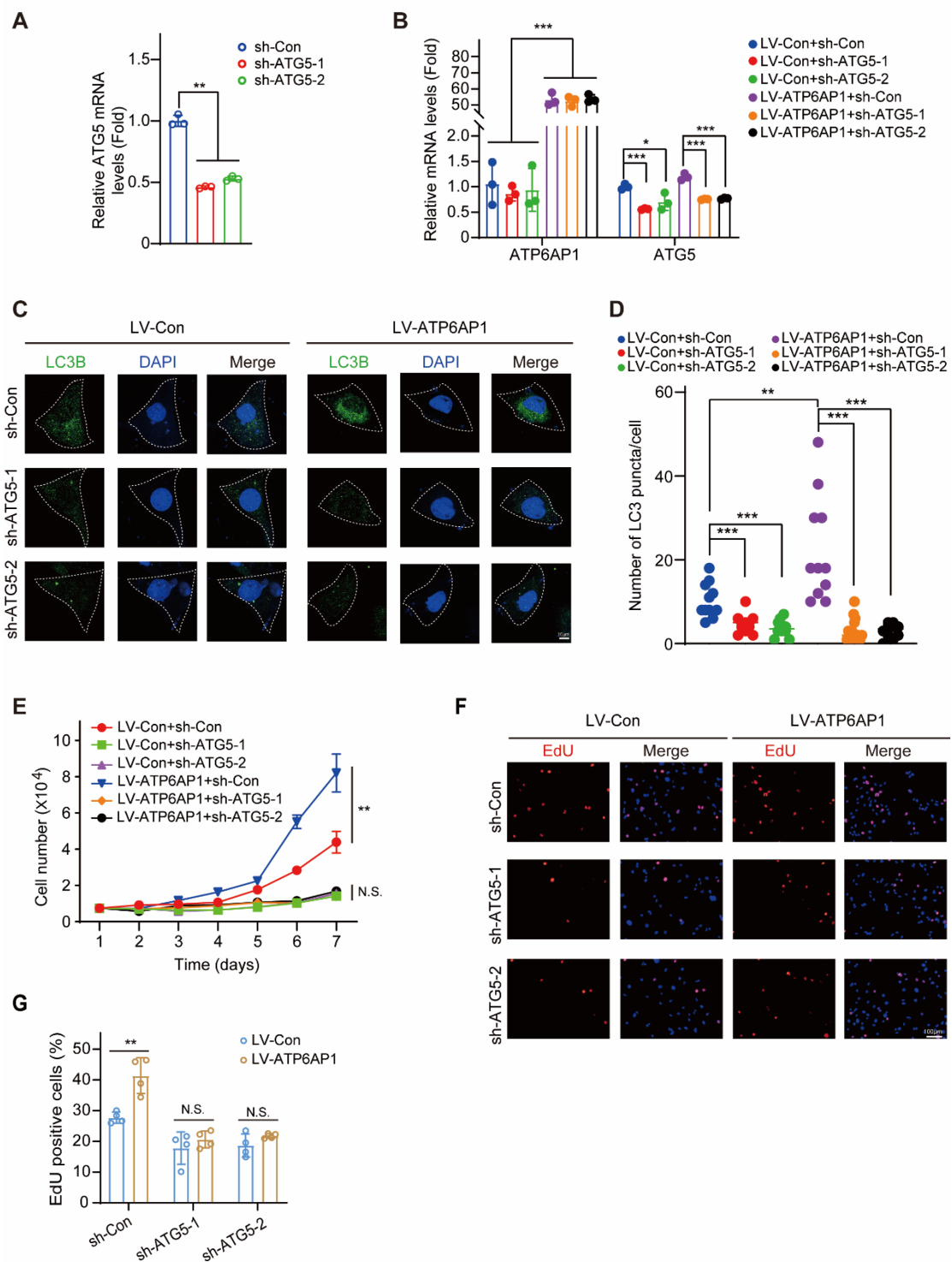


**Figure S5. Supplementary figure to Figure 6**

(A) RT-qPCR was used to verify the interference efficiency of ATG5 shRNA in ZR-75-1 cells. The bar graph displays the mean $\pm$ SD, n=3, \*\*p<0.01.

(B) T47D cells were infected with LV-ATP6AP1 and LV-sh-ATG5 lentiviruses

and harvested for RT-qPCR. The bar graph displays the mean $\pm$ SD, n=3, \* $p$ <0.05, \*\*\* $p$ <0.001.

(C) Knocking down ATG5 attenuated ATP6AP1- increased LC3 puncta. T47D cells infected with LV-ATP6AP1 or LV-sh-ATG5 were treated with EBSS for 4 hours. Representative immunofluorescence images of LC3 puncta were shown. Scale bars, 10 $\mu$ m.

(D) Quantification of LC3 puncta (volumetric pixels). Mean $\pm$ SD, \*\*\*  $p$  < 0.001, \*\*  $p$  < 0.01 by two-way ANOVA (n=10).

(E) ATP6AP1 facilitates luminal breast cancer cell proliferation by activating autophagy. T47D cells were infected with ATP6AP1 overexpression (LV-ATP6AP1) and ATG5 knockdown (LV-sh-ATG5) lentiviruses. Cell proliferation was determined by flow cytometry. The graph displays the mean $\pm$ SD, n=3, \*\* $p$ <0.01, N.S., no significance.

(F) Cell proliferation of T47D cells was determined by EdU assay. Scale bars, 100  $\mu$ m.

(G) Quantification of the data in (F). The bar graph displays the mean $\pm$ SD, n=3, \*\* $p$ <0.01, N.S., no significance.

**Supplementary Table 1: shRNAs used for knockdown of specific genes**

	Target sequences (5'-3')	Start
shRNA-ATP6AP1(#1)	5'-GCAGCTCTCTACCTACTTAGA-3'	232
shRNA-ATP6AP1(#2)	5'-ACAGTGACATTCAAGTTCATT-3'	974
shRNA-ATP6AP1(#3)	5'-GTCGCCTACTTCAATGCTTCC-3'	1073
shRNA-ATG5(#1)	5'-GATTCATGGAATTGAGCCAAT-3'	1010
shRNA-ATG5(#2)	5'-CAGGATGAGATAACTGAAAGG-3'	363

**Supplementary Table 2: Primers used for real-time PCR analyses**

ATP6AP1	Forward primer (5' to 3')	5'-CTTCTGGAATGACTCCTTTGCC-3'
	Reverse primer (5' to 3')	5'-ATTGCTGTGGACTTCGAGG-3'
ATG5	Forward primer (5' to 3')	5'-AAAGATGTGCTTCGAGATGTGT-3'
	Reverse primer (5' to 3')	5'-CACTTTGTCAGTTACCAACGTCA-3'
GAPDH	Forward primer (5' to 3')	5'-CACCAGGGCTGCTTTTAACTCTG-3'
	Reverse primer (5' to 3')	5'-GATTTTGGAGGGATCTCGCTCCTG-3'